NTIA Report 93-292

Wideband Propagation Measurements for Wireless Indoor Communication

Peter B. Papazian
Yeh Lo
Elizabeth E. Pol
Michael P. Roadifer
Thomas G. Hoople
Robert J. Achatz

U.S. DEPARTMENT OF COMMERCE
Barbara Hackman Franklin, Secretary

Gregory F. Chapados, Assistant Secretary
for Communications and Information

January 1993

TABLE OF CONTENTS

Page

LIST OF FIGURES

Page

LIST OF FIGURES

Page

TABLES

Page

WIDEBAND PROPAGATION MEASUREMENTS FOR WIRELESS INDOOR COMMUNICATION

Peter B. Papazian, Yeh Lo, Elizabeth E. Pol, Michael P. Roadifer,
Thomas G. Hoople, and Robert J. Achatz*

Wideband impulse response measurements were made to characterize proposed radio data channels in three indoor environments. The measurement system employed a 1.5 GHz carrier which was biphase shift key (BPSK) modulated using a 100 Mb/s pseudo-random code. By using a correlation receiver, the channel cophase and quadphase responses were measured and stored for later processing. Data processing included calculation of delay spread, correlation bandwidth (BW), and signal attenuation. The raw data are stored in binary form on tape and disk for further indoor propagation channel studies.

Key words: attenuation; BPSK; channel response; correlation bandwidth; delay spread; impulse response; indoor; propagation; radio; wideband

1. INTRODUCTION

The importance of wireless local area networks (WLAN) to the U.S. economy has led the Institute for Telecommunication Sciences (ITS) to implement a wideband measurement system to aid in standards development. This report presents a preliminary view of indoor channel propagation measurements and the metrology used in collection and analysis of indoor multipath interference data. Cumulative distributions of channel delay spread and correlation bandwidth have been calculated for three indoor environments. In addition, scatter plots of signal attenuation for these cases have been compiled. Because the raw data are stored as a time sequence of cophase and quadphase channel responses, they can still be used to extract additional information to characterize the indoor radio channel. It is hoped that the preliminary data processing effort can be expanded upon to facilitate the development of standards for WLAN equipment.

* The authors are with the Institute for Telecommunication Sciences, National Telecommunications and Information Administration, U.S. Department of Commerce, Boulder, CO 80303-3328.

2. MEASUREMENT SYSTEM

The ITS wideband probe is used to measure channel propagation characteristics. The system, which has a bandwidth of 1 GHz, has previously been used for outdoor millimeter wave propagation experiments in urban and vegetated settings (Violette et al., 1983, 1985, 1988). For indoor measurements, the probe was modified to transmit a 1.5 GHz carrier with BPSK modulation. The modulation code is a 127 bit pseudo-random sequence with bit rate adjustable between 100 and 500 Mb/s. Wideband, vertically polarized, omnidirectional antennas were used at the transmitter and receiver. The system measures cophase and quadphase channel response using a sliding correlator. By adjusting the sliding correlator's clock offset frequency, channel responses were measured every 100 ms and stored on a digital audio tape (DAT) recorder for later computer processing. A block diagram of the system is shown in Figures 1 and 2. The detector sensitivity is limited by its correlation noise level. The detector's dynamic range is determined by the 127 bit pseudo-random (PN) word length and is 42 dB. Dynamic range of the system is determined by the DAT recorder, which employed a 16 bit A/D converter with a range of 90 dB. By using variable gain video amplifiers in the DAT recorder, the signal voltage was maintained above the noise floor at all measurement sites.

3. DATA PROCESSING

The DAT medium allows complete storage of cophase and quadphase channel responses for 2 hours of continuous measurements. In our tests, the receiver was stationary while the transmitter was moved on a cart at a constant speed along a predetermined path. Data are stored in records that contained the two channels of digital data representing n discrete channel responses recorded for a predetermined path. A digital signal processing card is used to interface the DAT to a micro computer, which enables data transfer for processing and statistical analysis. Although impulses were collected every 100 ms, Doppler spread and coherence time were not included in the processing. This may be added in the future. However, we did include the ability to spatially average the data, which would minimize large variations in delay spread from individual scatterers.

The first step in processing is to separate the n distinct channel responses recorded on a particular data profile. To do this an autocorrelation is performed on the

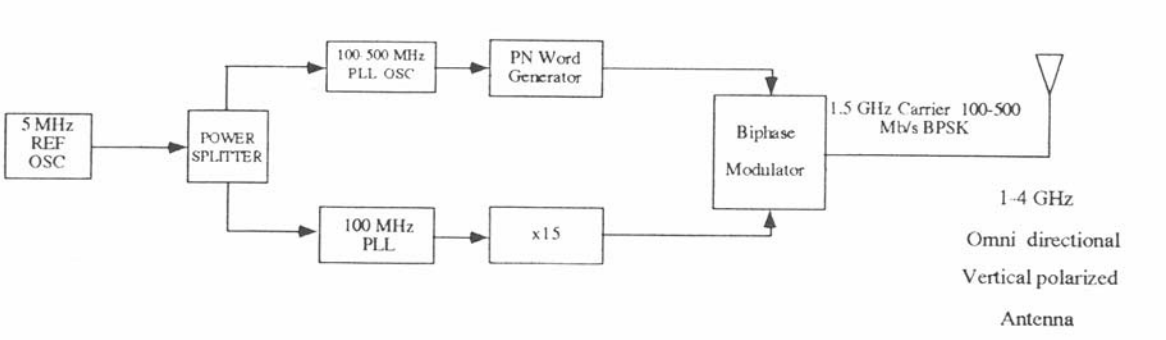

Figure 1. Wideband delay spread system transmitter.

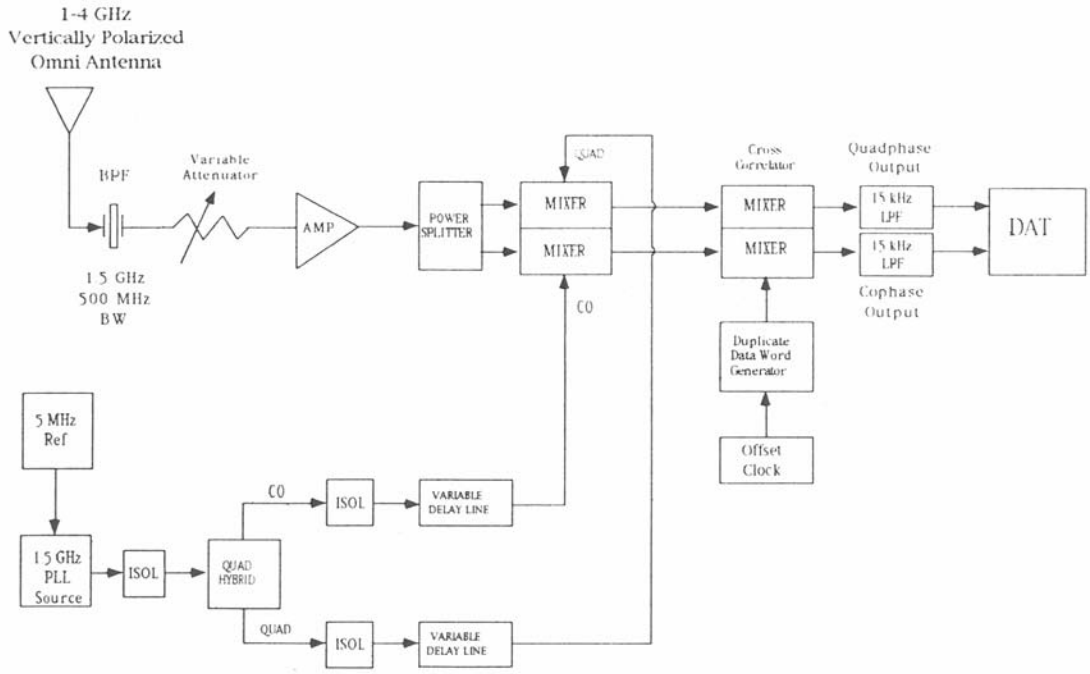

Figure 2. Wideband delay spread system receiver.

data to accurately determine the impulse repetition rate. Once this is accomplished, the peak of the first response (minus sufficient samples to account for the pulse rise time) is located to determine a beginning point of the record. Then the repetition rate is used to identify each succeeding response. Let $Co_i(\tau)$,(***i***=1,2..***n***) and $\boldsymbol{Quad_i}(\tau)$,(***i***=1,2..***n***) be the *n* distinct cophase and quadphase voltage time sequences for each channel of a data profile. The power-delay profile (PDP), $\boldsymbol{P_i}(\tau)$, is the channel impulse function squared. For the $\boldsymbol{i^{th}}$ record in a data profile, this is

$$P_i(\tau) = Co_i(\tau)^2 + Quad_i(\tau)^2. \qquad (1)$$

The PDP also can be averaged spatially by computing a running average of *k* adjacent impulse responses as the transmitter cart is moved, as shown in (2):

$$P_i^k(\tau) = \frac{1}{k}\sum_{\alpha=i}^{i+k-1} P_\alpha(\tau), \quad i = 1,\ 2,\ ...,\ j. \qquad (2)$$

The power delay is then normalized by total received power to obtain the averaged probability density function of excess delay, as in (3) (Cox, 1972, and Devasirvatham, 1987):

$$P_i^k(\tau) = \frac{P_i^k(\tau)}{\int_0^\infty P_i^k(\tau)\, d\tau}. \qquad (3)$$

The mean delay, $T0_i^k$**,** is then calculated using the statistical definition of first moment, as shown in (4):

$$T0_i^k = \int_0^\infty \tau p_i^k(\tau)\, d\tau. \qquad (4)$$

The delay spread Td_i^k is defined as the square root of the variance, which is also the square root of the second central moment, as shown in (5):

$$Td_i^k = \left[\int_0^\infty \left(\tau - T0_i^k\right)^2 p_i^k(\tau)\, d\tau\right]^{1/2}. \qquad (5)$$

This integral is performed as a summation with maximum integration time equal to the sum of the word lengths of the averaged impulses or up to the time for individual impulses when the signal decays to a predefined threshold level.

The signal loss versus distance is also tabulated. This quantity is normalized to 0 dB with the transmitter and receiver separated by 3 m. The loss is calculated using the sum power or energy per impulse which is the integral of the PDP, as in (6). This is also the average continuous wave (cw) power over the system bandwidth.

$$P_{i_{Sum}}^{k} = \int_{0}^{\infty} P_i^k(\tau)\, d\tau. \qquad (6)$$

The correlation function (Proakis, 1983) is the Fourier transform of the probability density function,

$$R(\Delta f) = F[[p_i^k(\tau)]]. \qquad (7)$$

The correlation bandwidth is then defined as the bandwidth at which the correlation drops by 50 percent.

4. CALIBRATION

System calibration and delay spread processing algorithms were checked using two coaxial transmission lines to simulate a multipath signal in the laboratory. The calibration setup is shown in Figure 3. The delta time for signal arrival was calculated using cable manufacturer specifications. The attenuation of a 1.5 GHz cw signal by these delay lines was also measured. These results are listed in Table 1. Figure 4 shows the measurement results for one nonaveraged impulse response from a 10 second calibration test. Table 2 lists the measurement results verses the known characteristics of the unequal delay lines. Delay measurements for a random impulse were found to be accurate to about 5 percent and amplitude measurements agreed to about 7 percent.

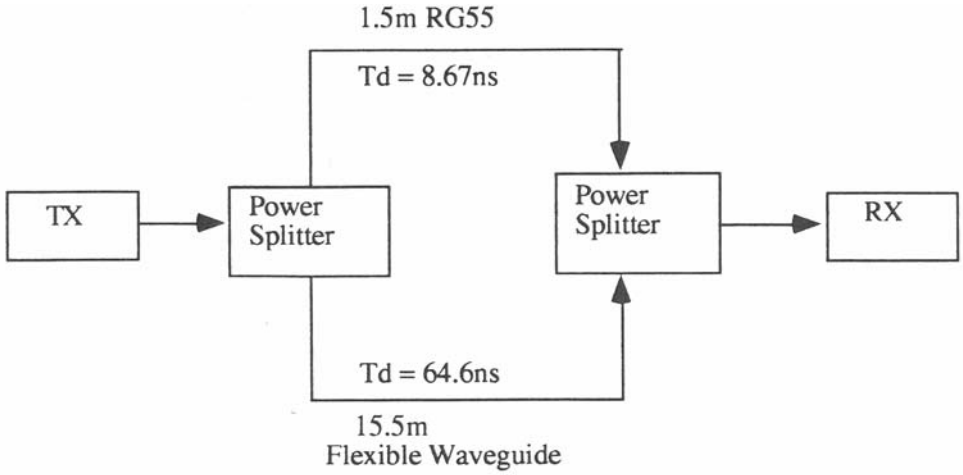

Figure 3. Calibration test setup.

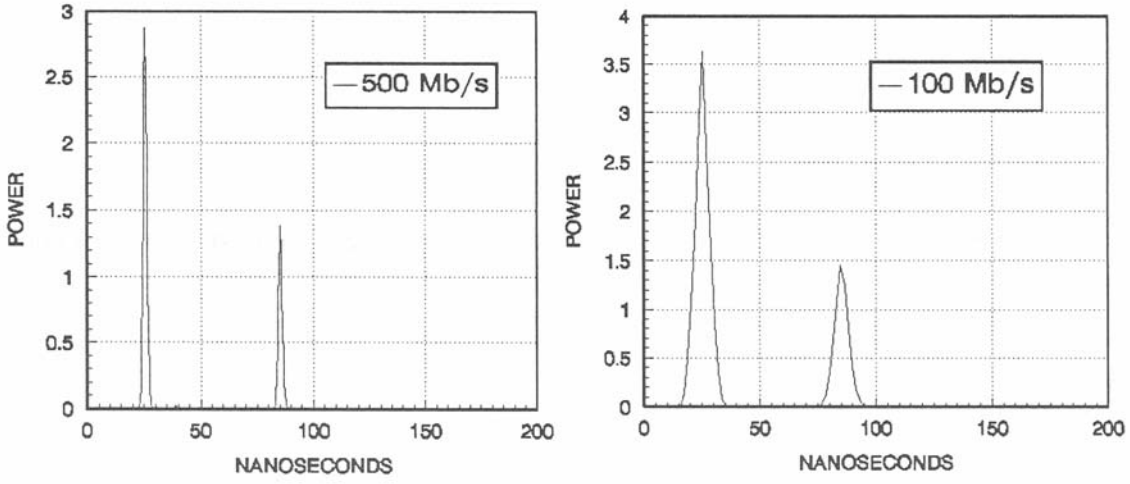

Figure 4. Measured calibration data. Single correlation at 100 and 500 Mb/s, 60 ns delay.

Table 1. Delay Line Characteristics at 1.5 GHz

Cable #	V_p(m/s)	L(m)	T_d(ns)	A(dB)
1 (FWG)	2.40E+8	15.5	64.6	-5.67
2(RG55)	1.73E+8	1.5	8.67	-2.17

Table 2. Calibration Results for Known Delay Δt and Peak Signal Attenuation ΔA Measured at 100 Mb/s and 500 Mb/s

	Calculated	Measured 100, 500 Mb/s	Percent Error 100, 500 Mb/s
Δt (ns)	55.9	59, 58	5.5, 3.7
ΔA (dB)	3.45	3.417, 3.483	7.3, 7.3

A minimum delay spread measurement was also made. To do this, a delay spread profile for a direct signal with no multipath was recorded for 10 s. The theoretical minimum delay spread for the system under these conditions was calculated for a triangular pulse 127 bits high with a base 2 bits wide. A threshold detection level of 20 dB was then used to perform the integration required in equation (5). Results from this test are given in Table 3.

Table 3. Measured Versus Calculated Minimum Delay Spreads for Direct Signal at 100 and 500 Mb/s Using a 20 dB Threshold

	Calculated (ns)	*Measured* (ns)
T_{d100}	4.2	3.6
T_{d500}	0.8	1.1

5. MEASUREMENT RESULTS

Delay spread measurements were made at three locations. Site #1 was a long hallway with cinder block walls at the Department of Commerce Boulder Laboratories. The hallway was flanked by offices on one side and laboratories on the other. Site #2 was the Commerce auditorium, also located at the Boulder Laboratories. This room is wood paneled with metal seats, and a raised stage area. Site #3 was an open floor plan office with soft partitions at the US West Research Facility in Boulder, CO. Floor plans, transmitter, receiver, and data profile locations are shown in Figures 5, 6, and 7. In all cases, the transmitter was moved on a cart along the profiles with a fixed receiver location. The receiver was positioned at a height of 2.1 m (7 ft). The transmitter height was 1.6 m (5.3 ft). This gave a clear line of sight (LOS) between the transmit and receive antennas in Site #1 and Site #2. In Site #3, the soft partitioned office, all profiles except 1 and 2 were obstructed line of sight (OLOS). Obstructions included soft partitions, which were 6 ft high and randomly spaced office furniture (see Figure 6).

Delay spreads were calculated from the received PDP using no averaging and a 20 dB threshold. Signal levels below threshold (20 dB below the peak signal) on a PDP are set to zero. This must be done so delay spread is not a function of integration time.

Because significant delays were encountered at the US West office on OLOS profiles, the 100 Mb/s data were selected for reporting. This choice was made by monitoring the tail of each PDP. The ratio of the average value of the tail of the PDP and

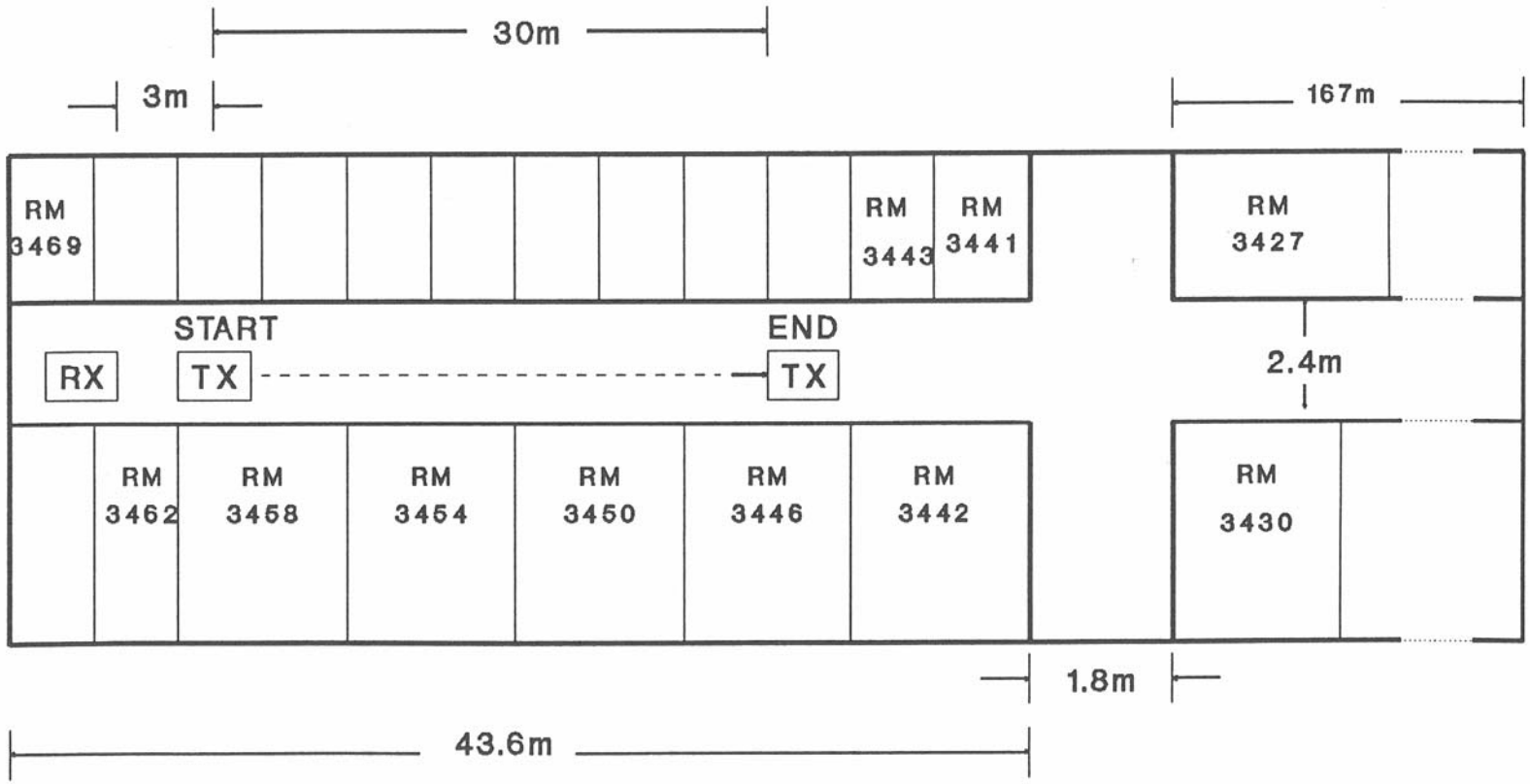

Figure 5. Site #1 floor plan and data profile, Wing 4 hallway, Radio Building, not to scale.

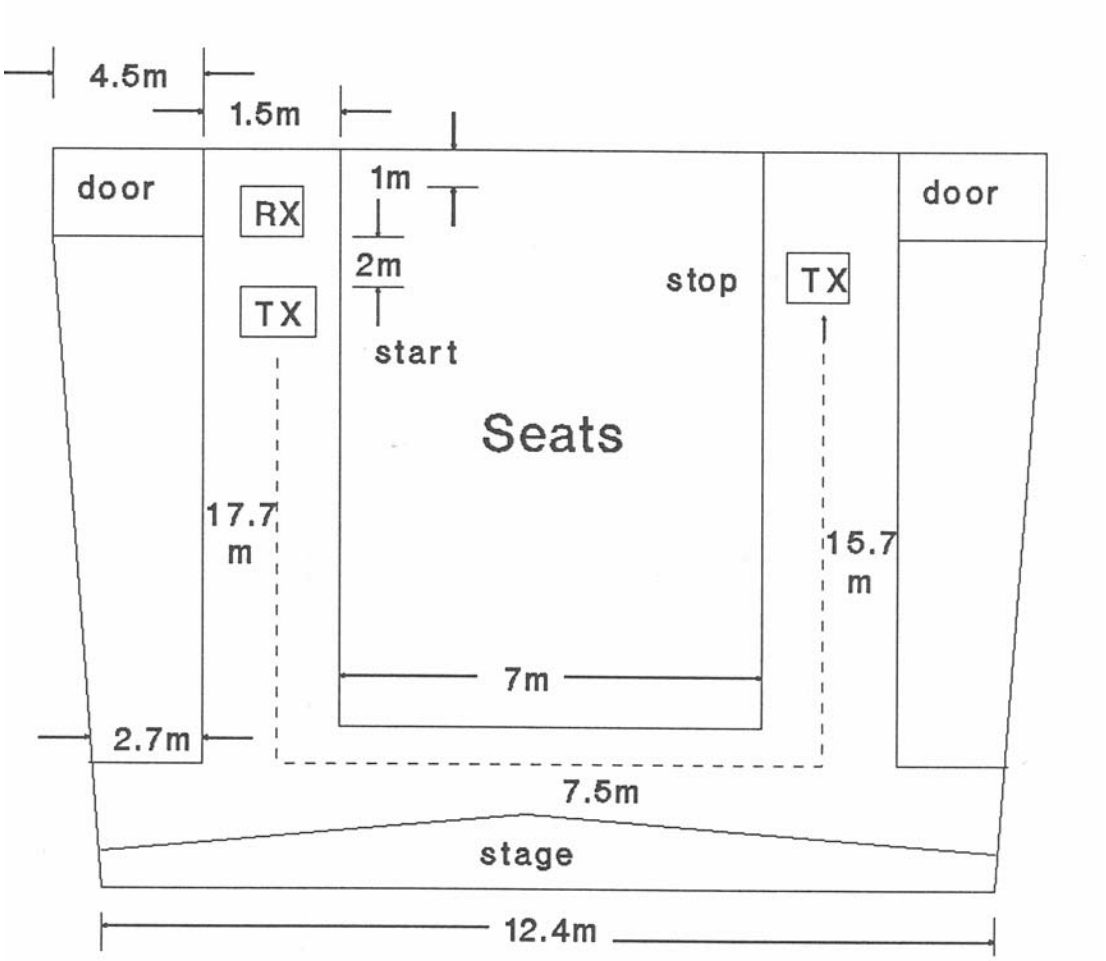

Figure 6. Site #2 floor plan, Radio Building auditorium.

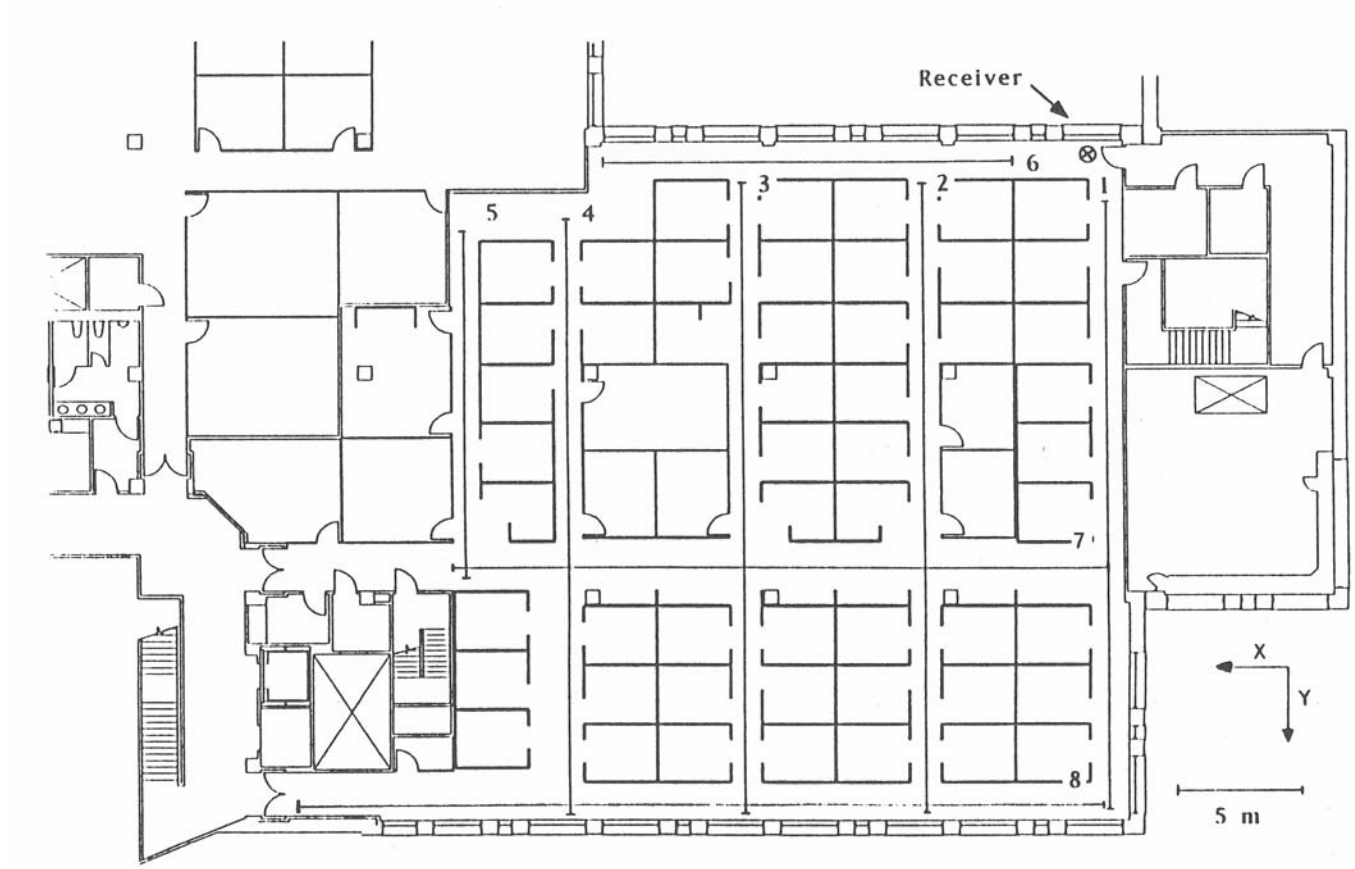

Figure 7. Site #3 US WEST Room 3200 floor plan with eight delay spread profile locations and receiver location.

the peak signal of each PDP should be at least 20 dB. An example of this calculation is shown in Figure 8 and is labeled PDP Amplitude Ratio. The delay profile and PDP's associated with the minimum and maximum delay spreads for US West profile 4 are also shown in Figure 8. The correlation function for the maximum-minimum impulses from Figure 8 are shown in Figure 9. As can be seen in Figure 9, correlation function's of PDP's with longer delays decay more rapidly to their 3 dB points. Since the PDP's are real, only the positive frequencies of their correlation functions are displayed. To find the correlation bandwidth, the 3 dB point for positive frequencies, f^+, is doubled. It can be seen in Figure 9 that the two sided correlation BW does not have a precisely universe relationship with its delay spread. For comparison of these results with calibration data, the 3 dB points for direct signals with no delay spread are given in Table 4.

Table 4. System Bit Rate Versus Measured 3 dB Point of Correlation Function for a Direct Signal

Bit Rate (Mb/s)	100	200	500
3 *dB Point(MHz)*	112	225	450

When making estimates of the correlation BW, the 3 dB points from Table 4 can be considered as upper limits for channel BW measurements. Correlation BW's approaching these numbers are really underestimates for the channel. To correct this, the system transfer function can be deconvolved in the processing. This would extend the usable correlation BW measurement ability of the system. This has not been done, but can be if these upper limits are considered important.

Delay spread, correlation BW, and attenuation versus position graphs have been compiled for all data profiles. These graphs display the calculated results for each PDP at 100 ms intervals again using a 20 dB threshold and no spatial averaging. The time sequence was then converted to distance by assuming a constant cart speed. This sampling rate and cart speed gave approximately five delay spread measurements per carrier wavelength.

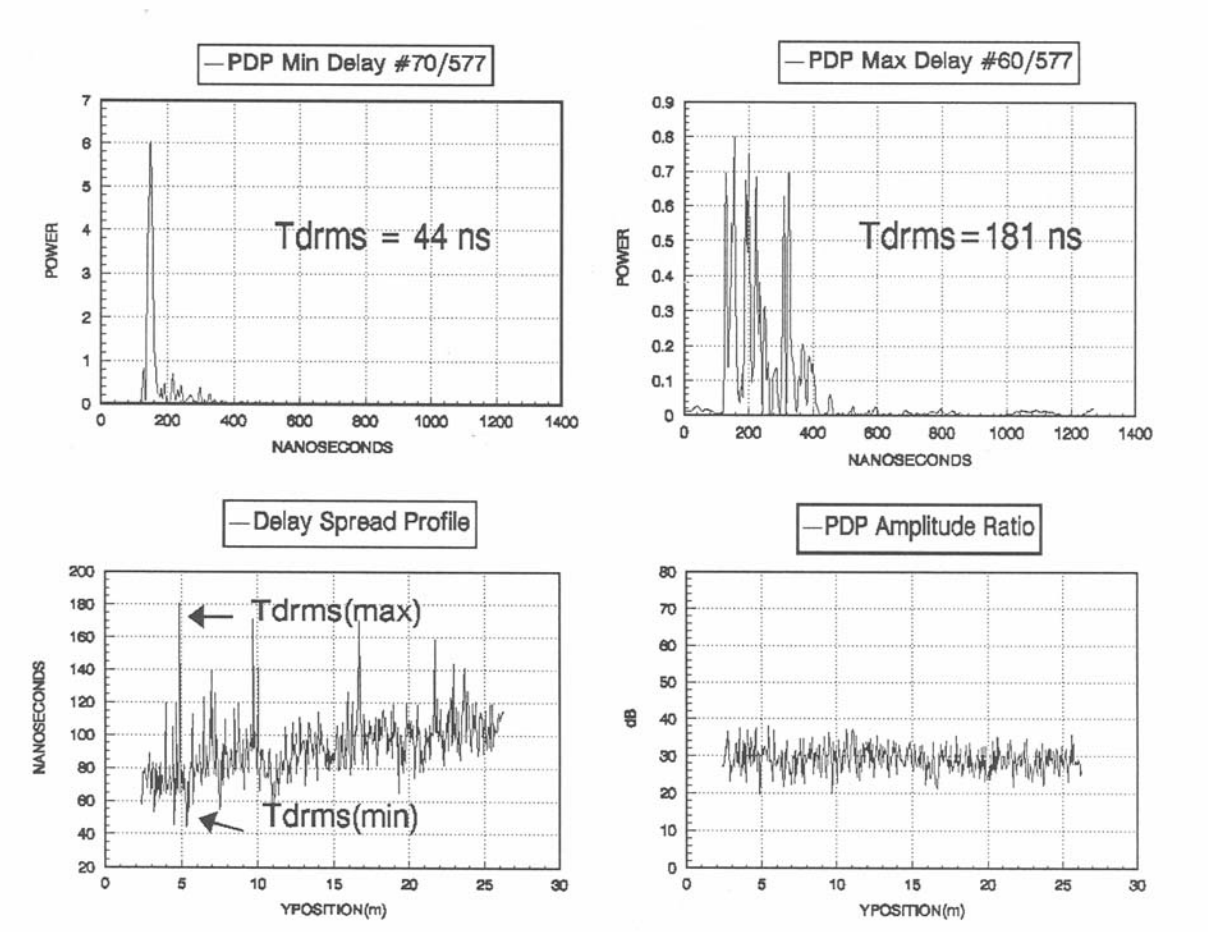

Figure 8. US WEST Profile No. 4, PDP's of max, min delay spreads, delay spread profile, and PDP amplitude ratio.

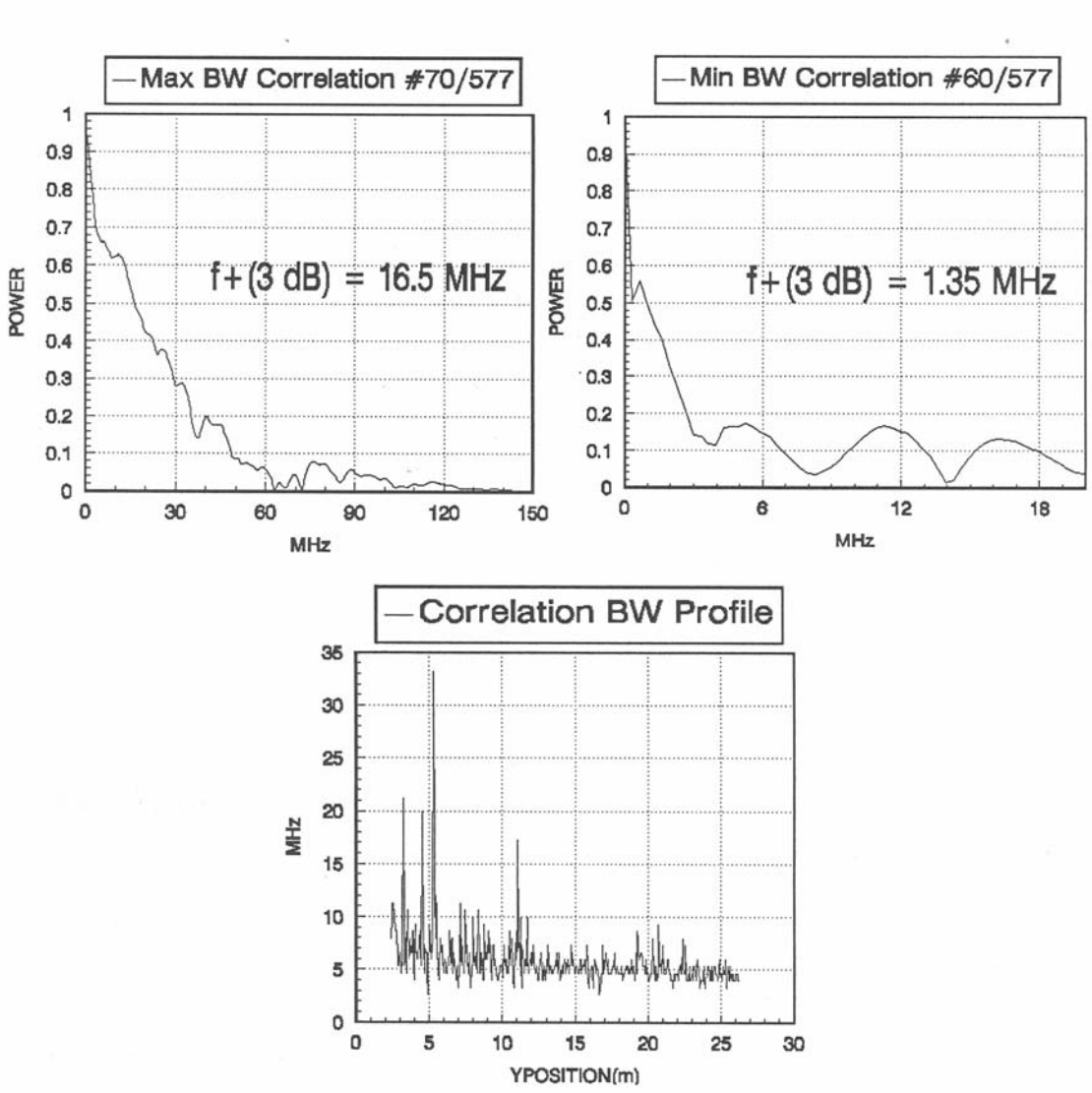

Figure 9. US WEST Profile No. 4, positive frequency correlation functions for min and max PDP delay spreads, correlation BW ($2f^{+}$) profile.

Figures 10, 11, and 12 are comparisons of delay spread profiles and correlation BW. Figure 10 shows the two LOS profiles at the US WEST office. Figure 11 displays the OLOS profiles from US WEST, and Figure 12 shows the LOS profiles measured at the Department of Commerce (DOC) sites. The somewhat inverse relationship between delay spread and correlation BW can be seen on all plots. In general, the delay spread magnitudes are dominated by the geometry of the measurement site. For LOS paths delay spread decreases slightly with increasing distance in the narrow DOC hallway (Figure 13) and has smaller delay spreads than the LOS measurements in the square plan auditorium (Figure 13). LOS paths in the US WEST office experience larger delay spreads of up to 70 ns caused by possible multipath through windows and scattering, diffraction, and reflections from partitions and office furniture.

OLOS paths at US WEST (Figure 11) exhibit the largest delays, which increase somewhat linearly with distance. Here we see maximum delay spreads around 200 ns on profiles 2, 3, 4, 5, 7, and 8.

Cumulative distributions functions (CDF's) and histograms of delay spread were compiled and are shown in Figures 14, 15, and 16. Median values of delay spread are 8.5, 24, and 65 ns for the hallway, auditorium, and soft partitioned office, respectively. The US WEST data shows bi-modal distributions due to the combination of LOS and OLOS profiles. To resolve this, US WEST LOS and OLOS data were separated and used to calculate independent CDF's and histograms of delay spread and correlation BW. These data are shown in Figures 17, 18, 19, and 20.

Position data were then used to convert attenuation versus profile position to attenuation versus log euclidean distance (Alexander, 1982) from the transmitter. Scatter plots were made for each profile, and the average slope was determined using a linear regression algorithm. Results are given in Figures 21, 22, and 23, and the average power law coefficients are summarized in Table 5.

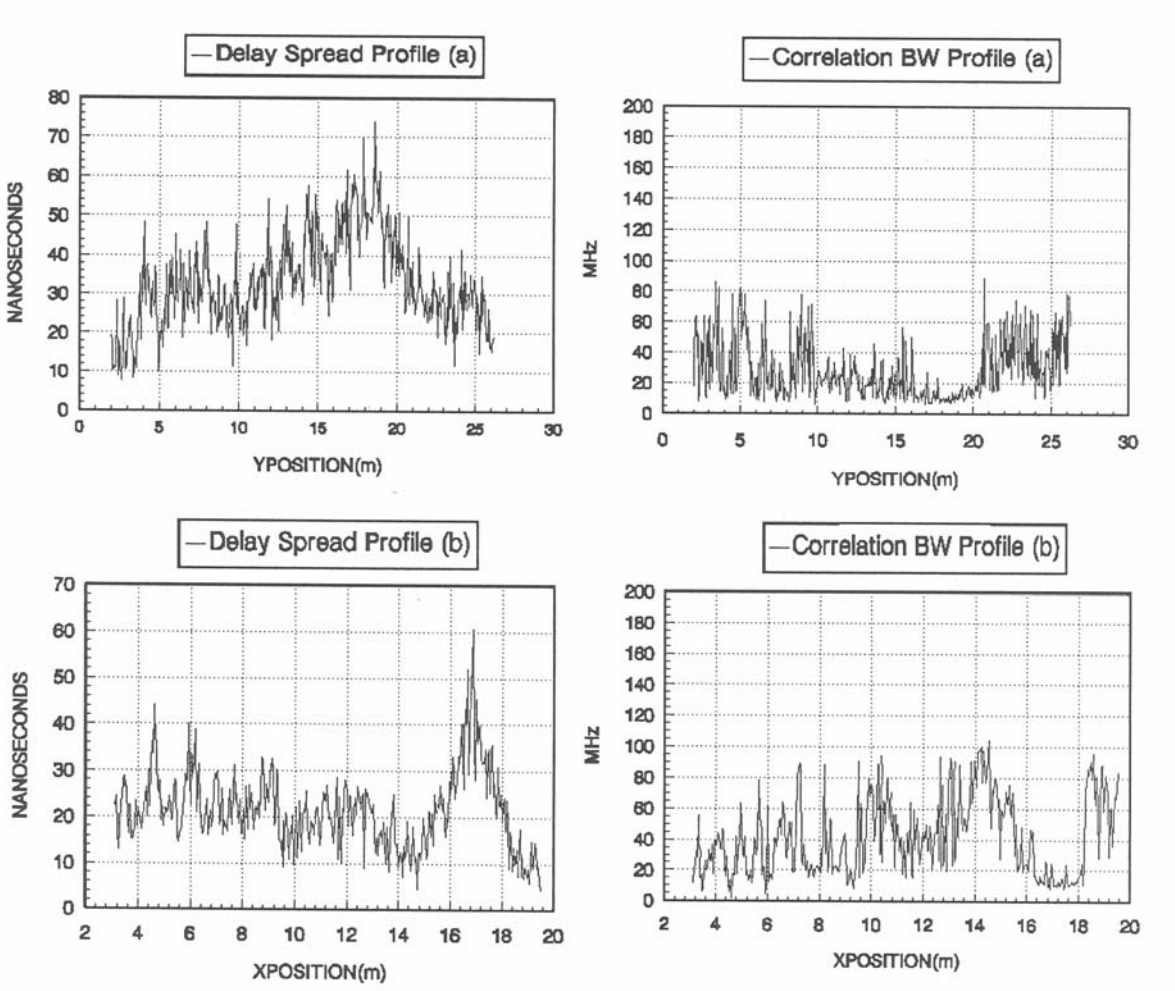

Figure 10. Delay spread and correlation BW profiles. US WEST Rm. 3200 (LOS): Profiles (a) 1 and (b) 6.

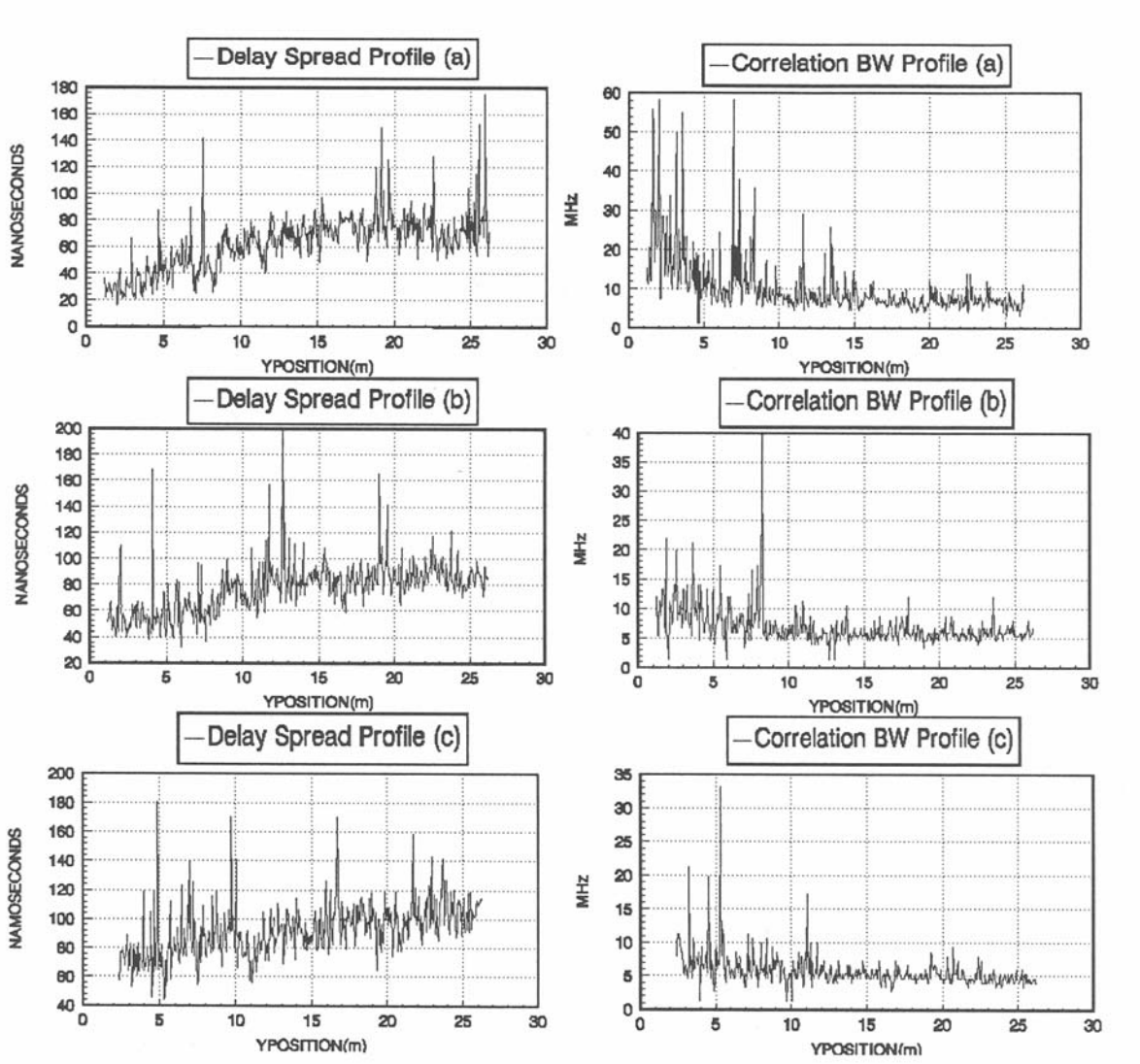

Figure 11. Delay spread and correlation BW profiles. US WEST Rm. 3200 (OLOS): Profiles (a) 2, (b) 3, and (c) 4.

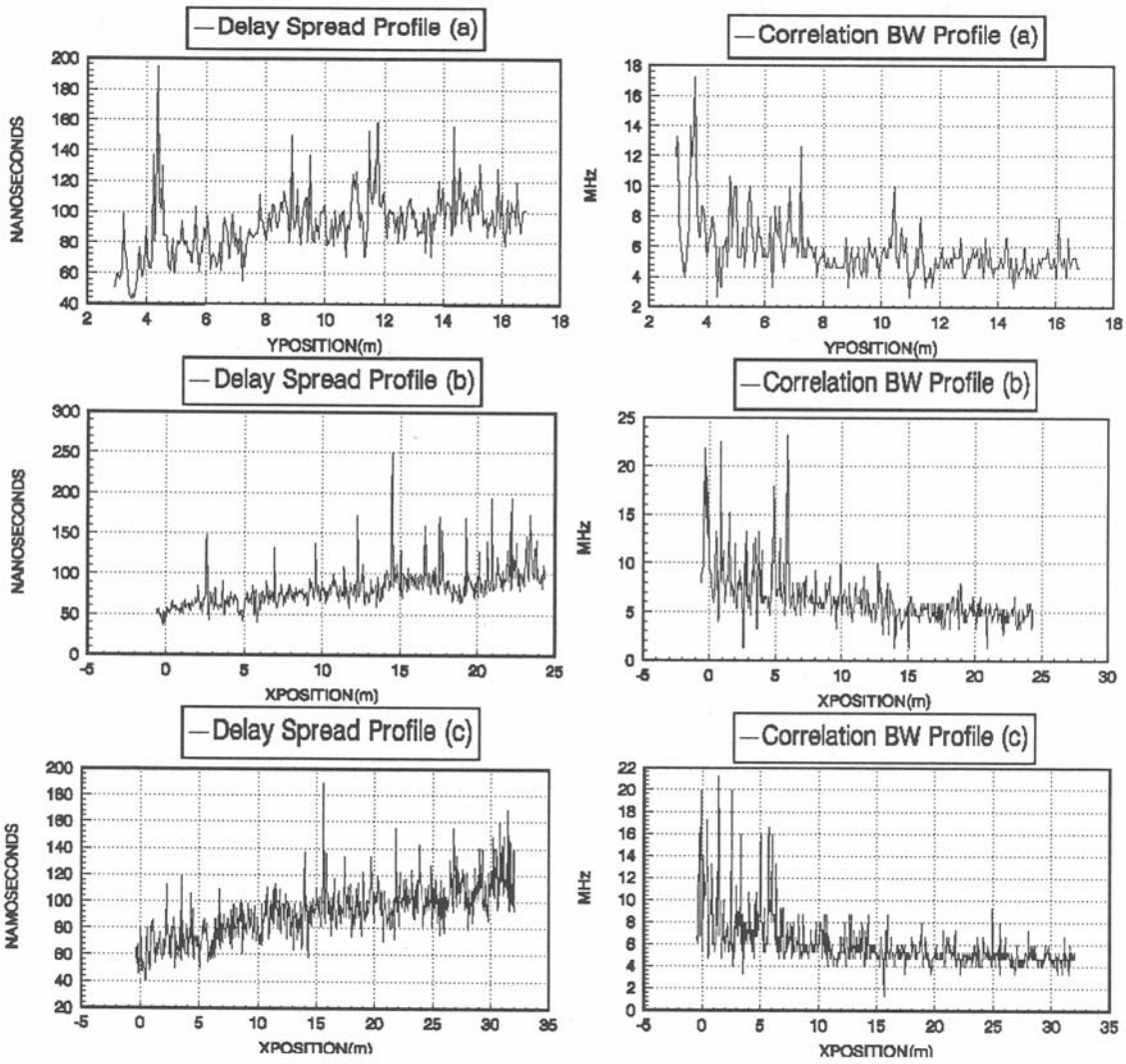

Figure 12. Delay spread and correlation BW profiles. US WEST Rm. 3200 (OLOS): Profiles (a) 5, (b) 7, and (c) 8.

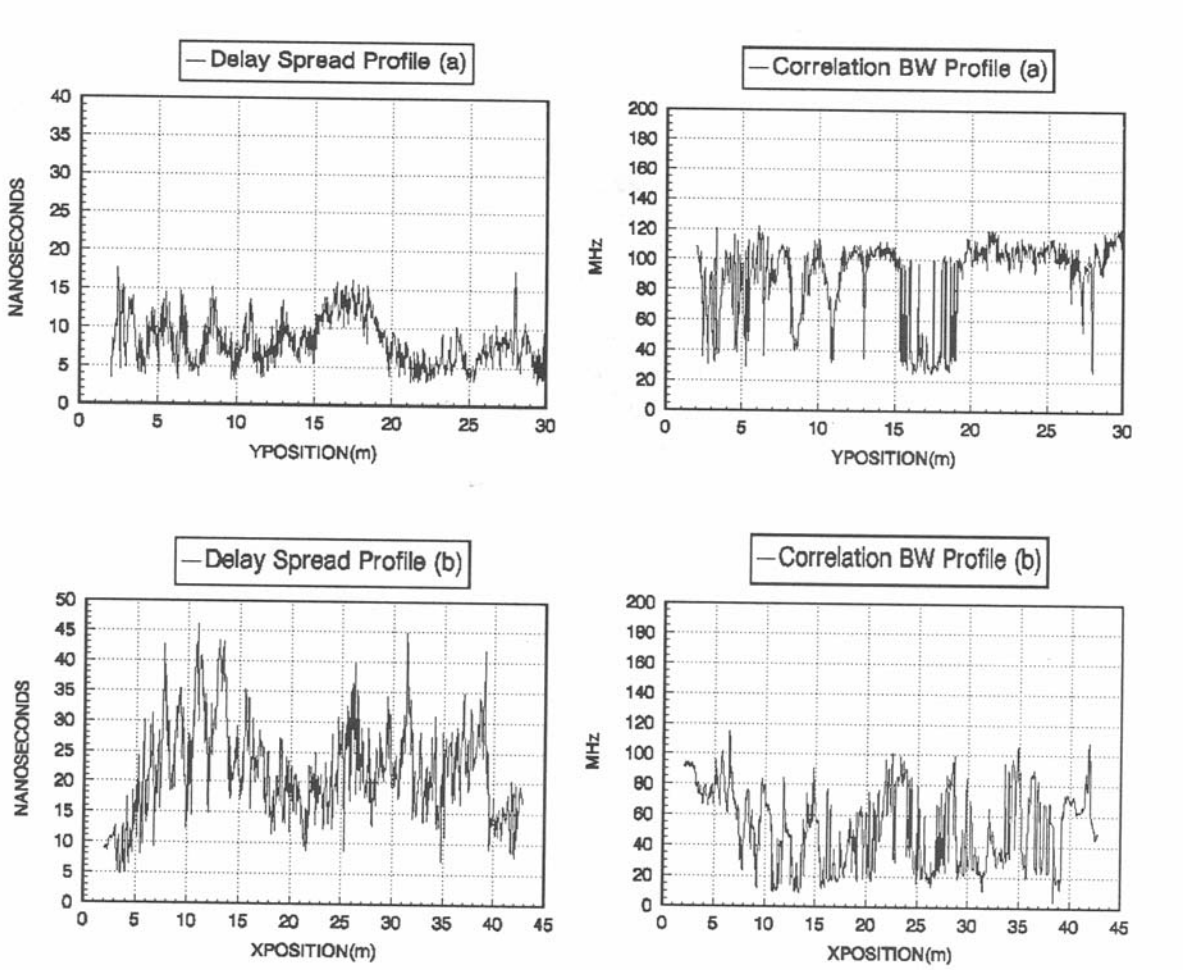

Figure 13. Delay spread and correlation BW profiles. Commerce Radio Building (LOS): (a) hallway and (b) auditorium.

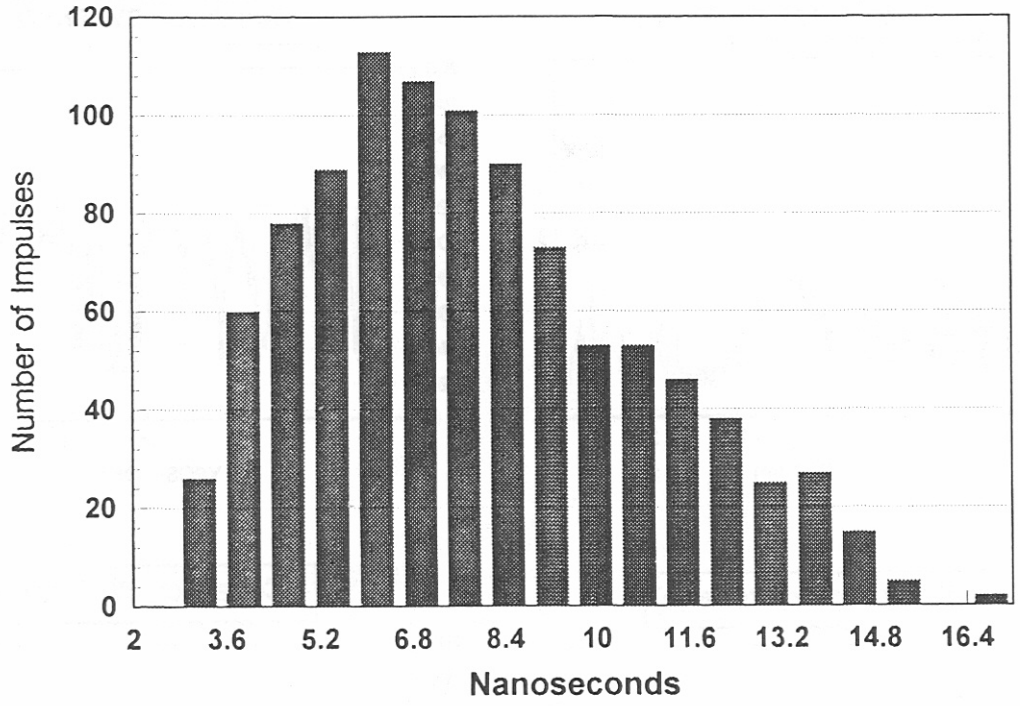

Figure 14a. Histogram of delay spreads, Commerce hallway.

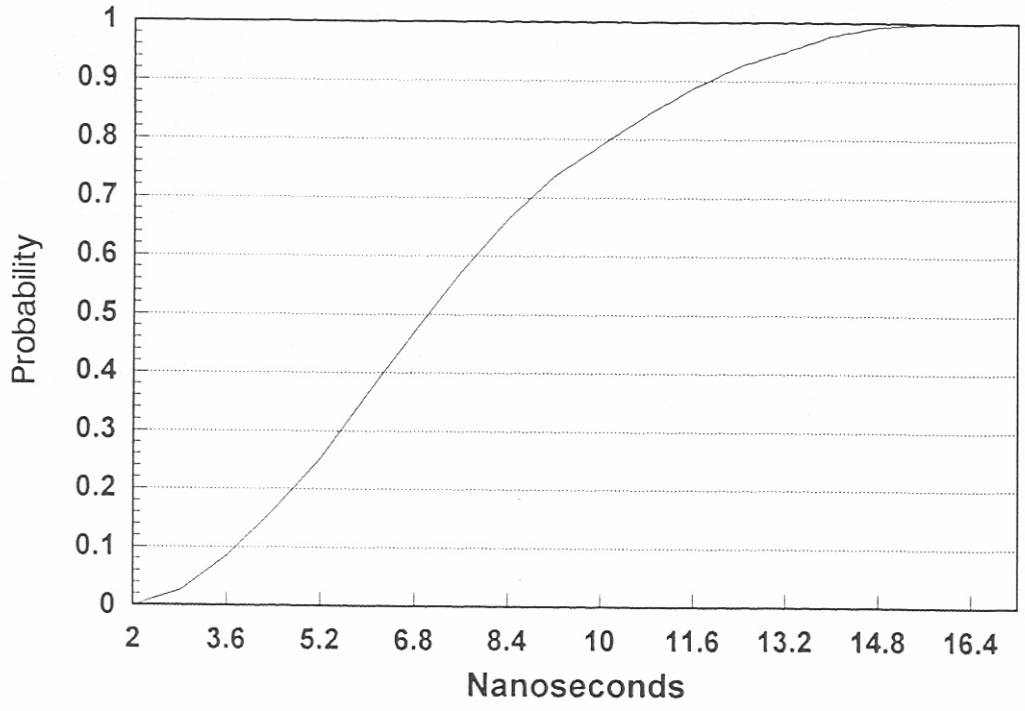

Figure 14b. CDF of delay spreads, Commerce hallway.

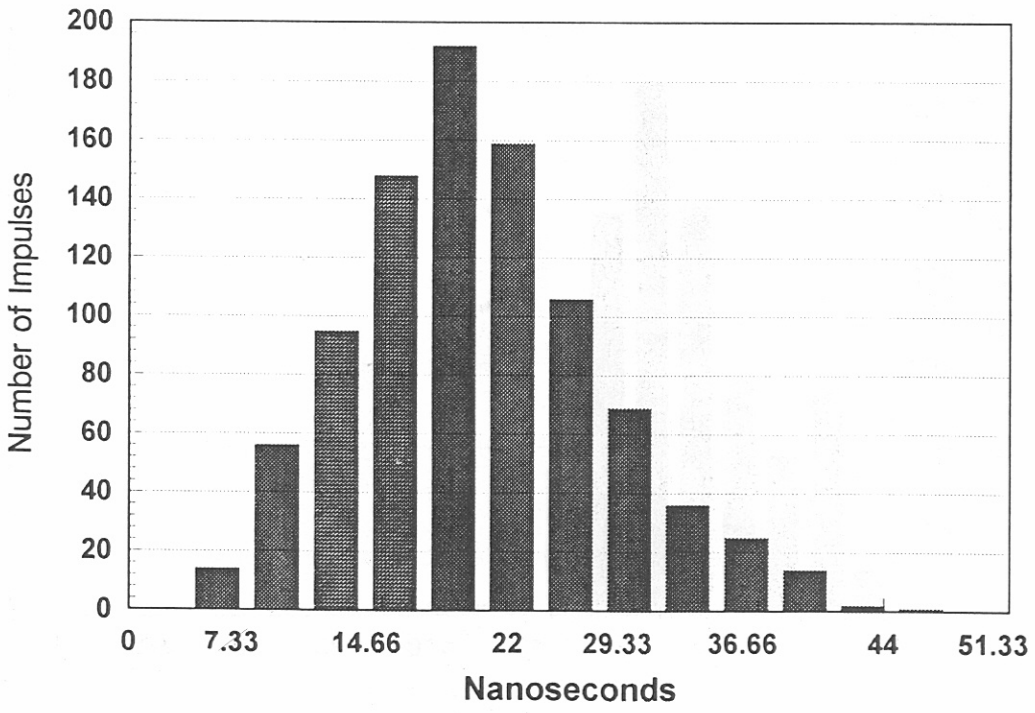

Figure 15a. Histogram of delay spreads, Commerce auditorium.

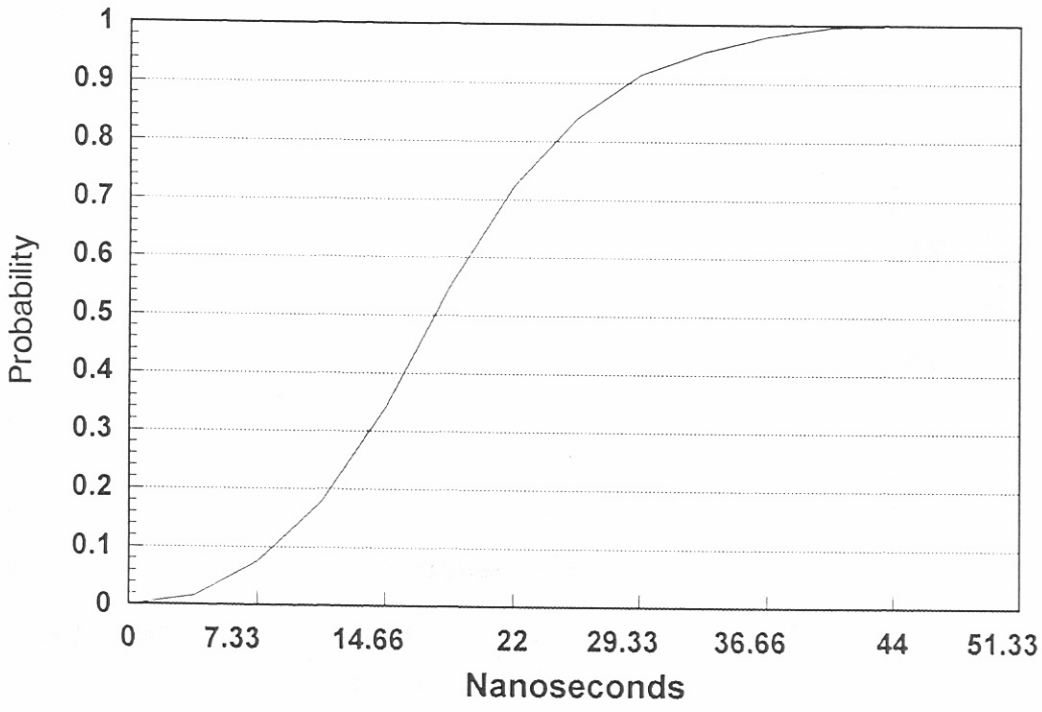

Figure 15b. CDF of delay spreads, Commerce auditorium.

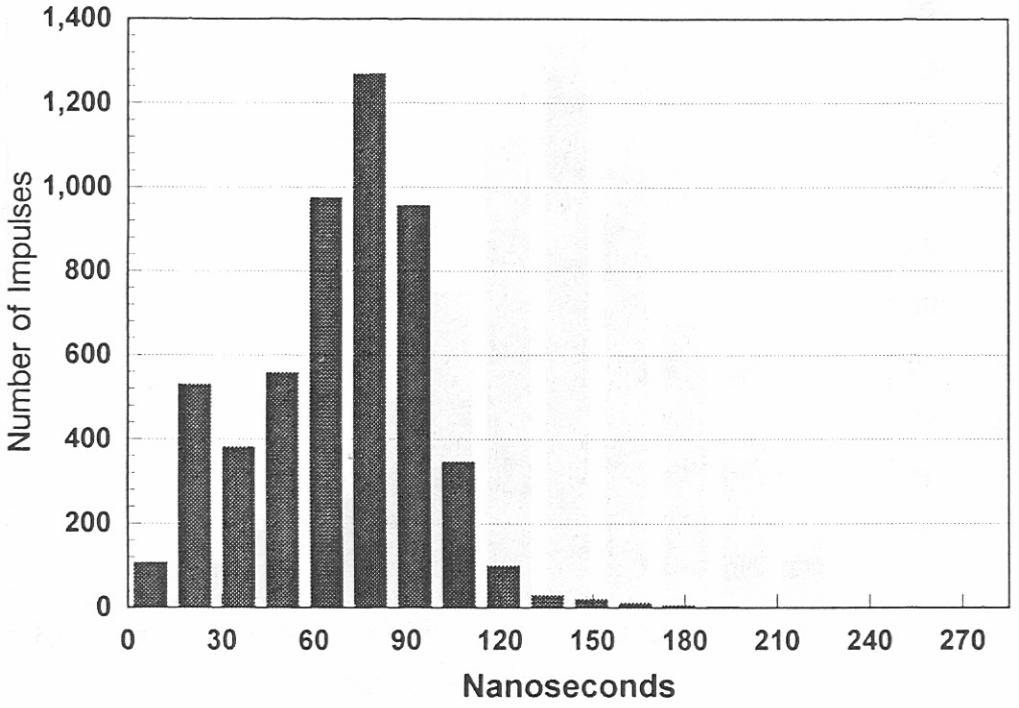

Figure 16a. Histogram of delay spreads, US WEST office.

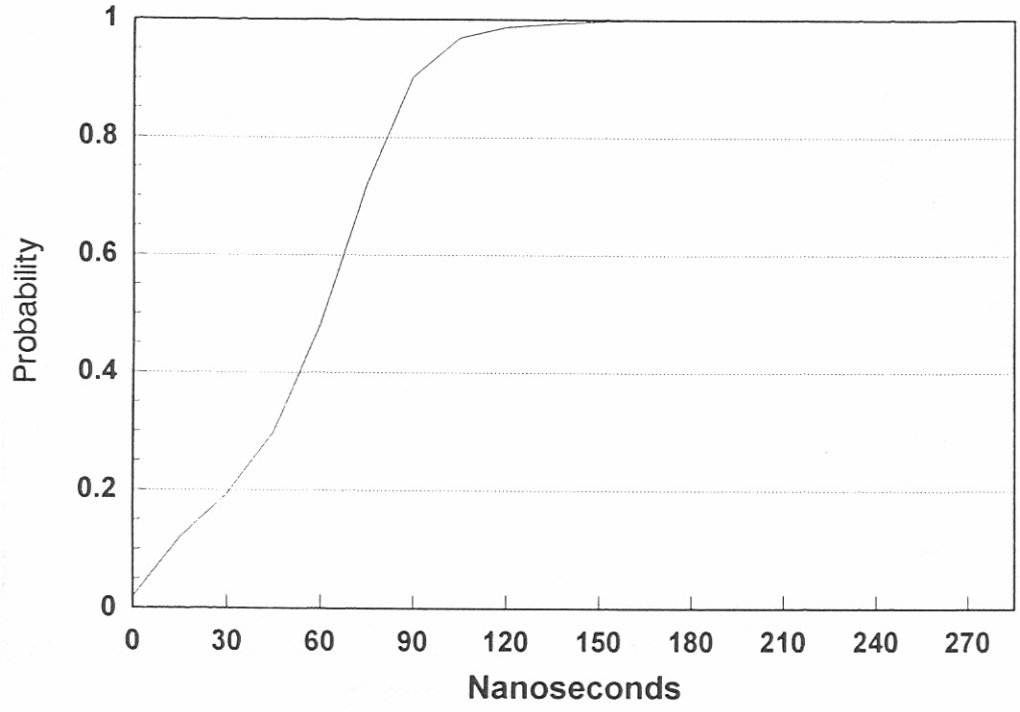

Figure 16b. CDF of delay spreads, US WEST office.

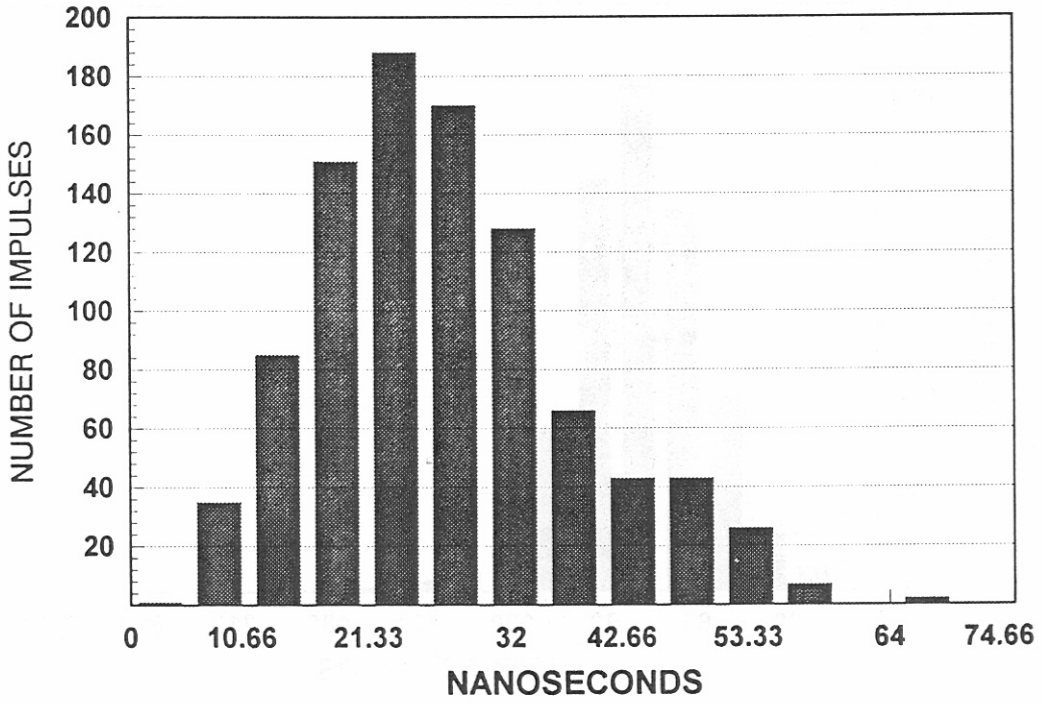

Figure 17a. Histogram of delay spreads, US WEST, LOS profiles 1 and 6.

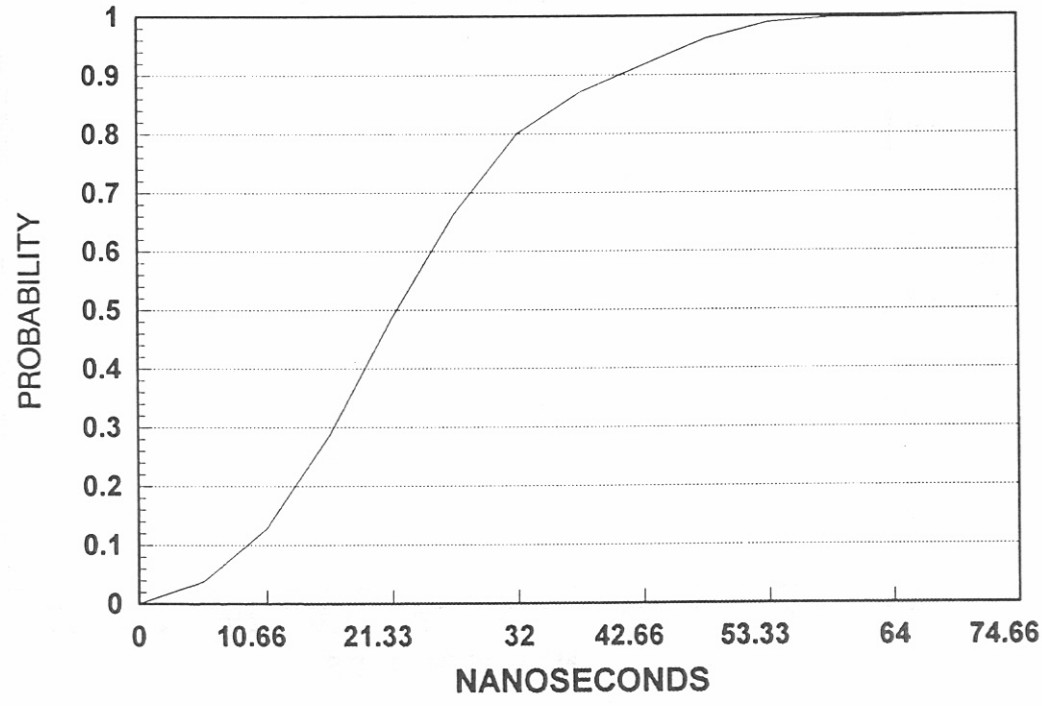

Figure 17b. CDF of delay spreads, US WEST, LOS profiles 1 and 6.

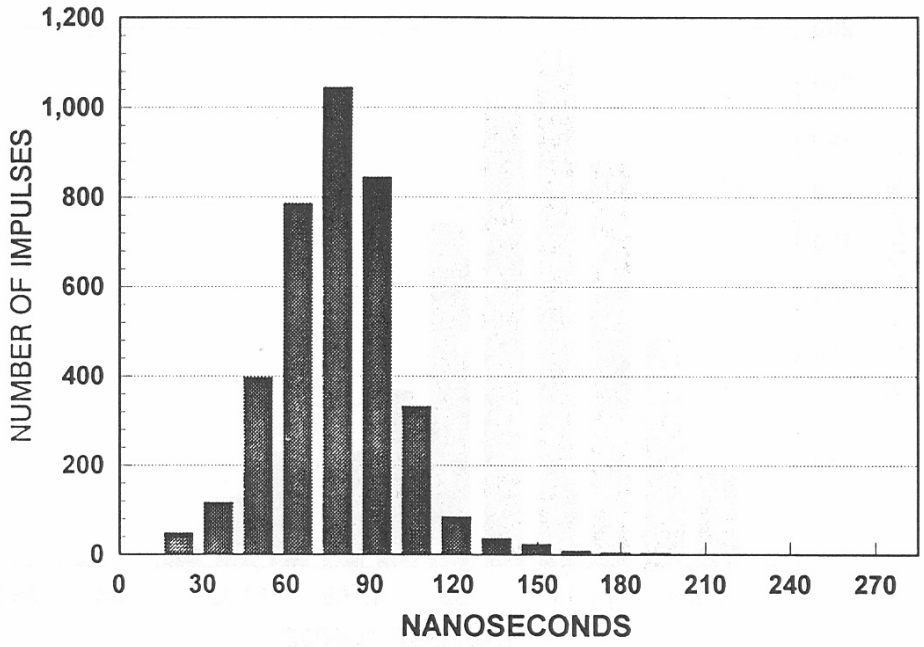

Figure 18a. Histogram of delay spreads, US WEST, OLOS profiles 2, 3, 4, 5, 7, and 8.

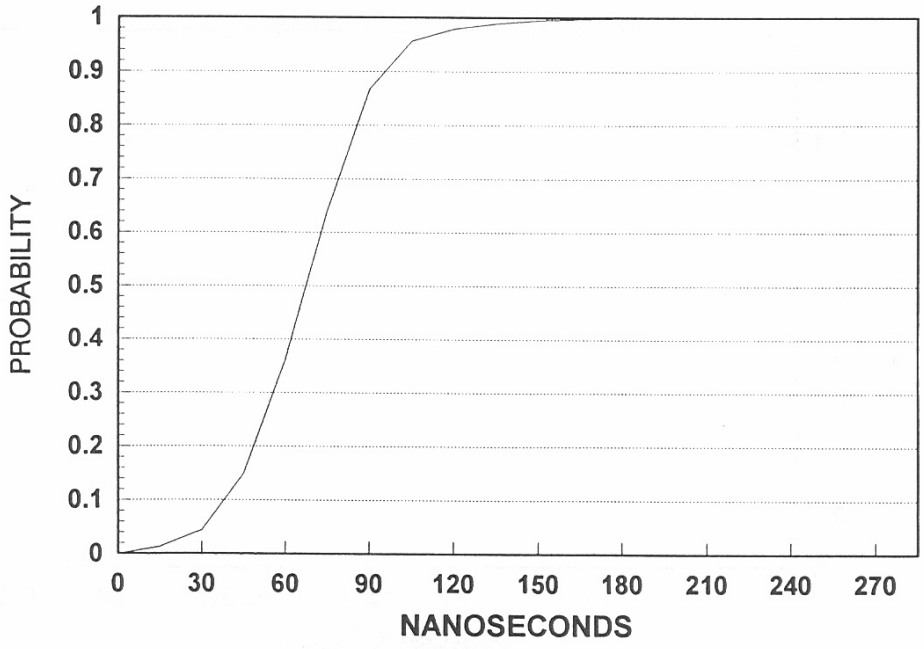

Figure 18b. CDF of delay spread, US WEST, OLOS profiles 2, 3, 4, 5, 7, and 8.

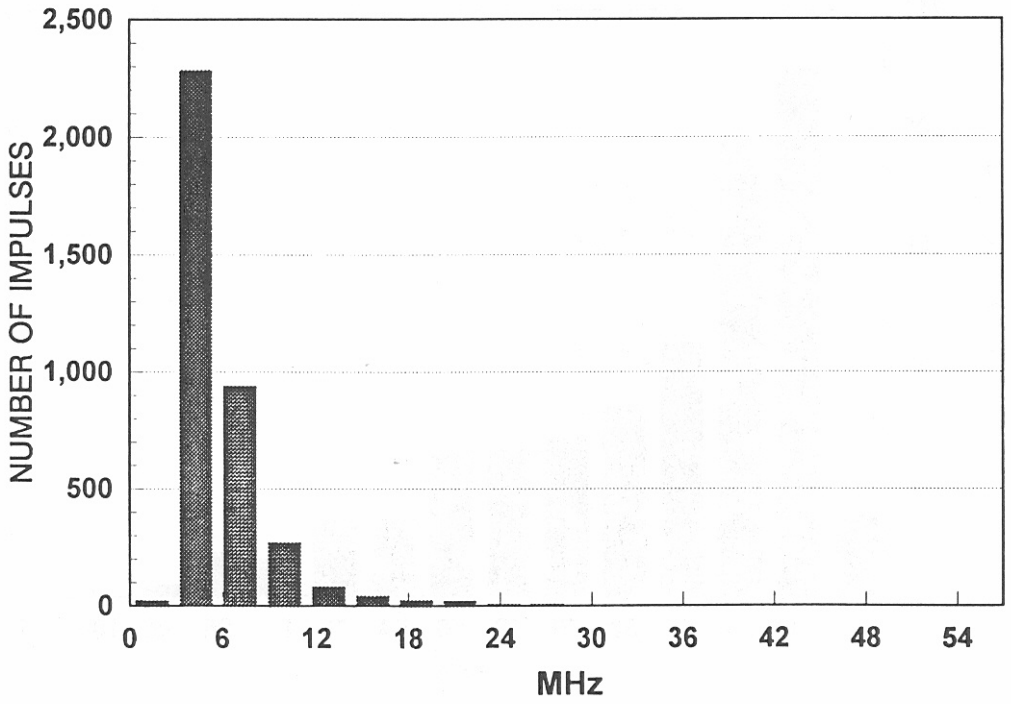

Figure 19a. Histogram of correlation BW, US WEST OLOS profiles.

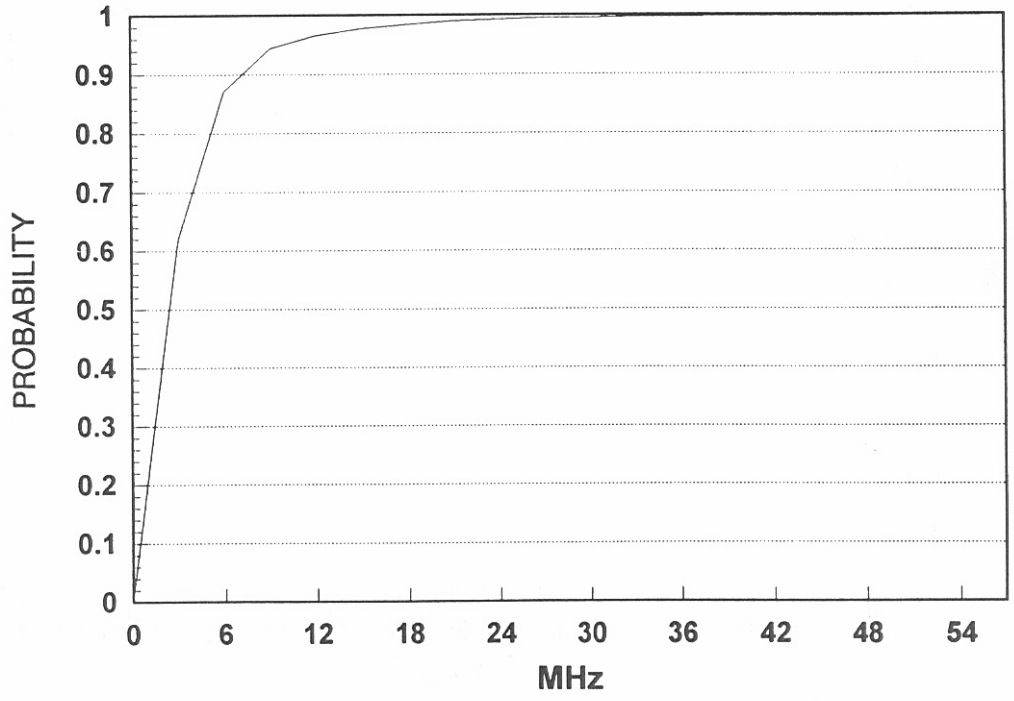

Figure 19b. CDF of correlation BW, US WEST, OLOS profiles.

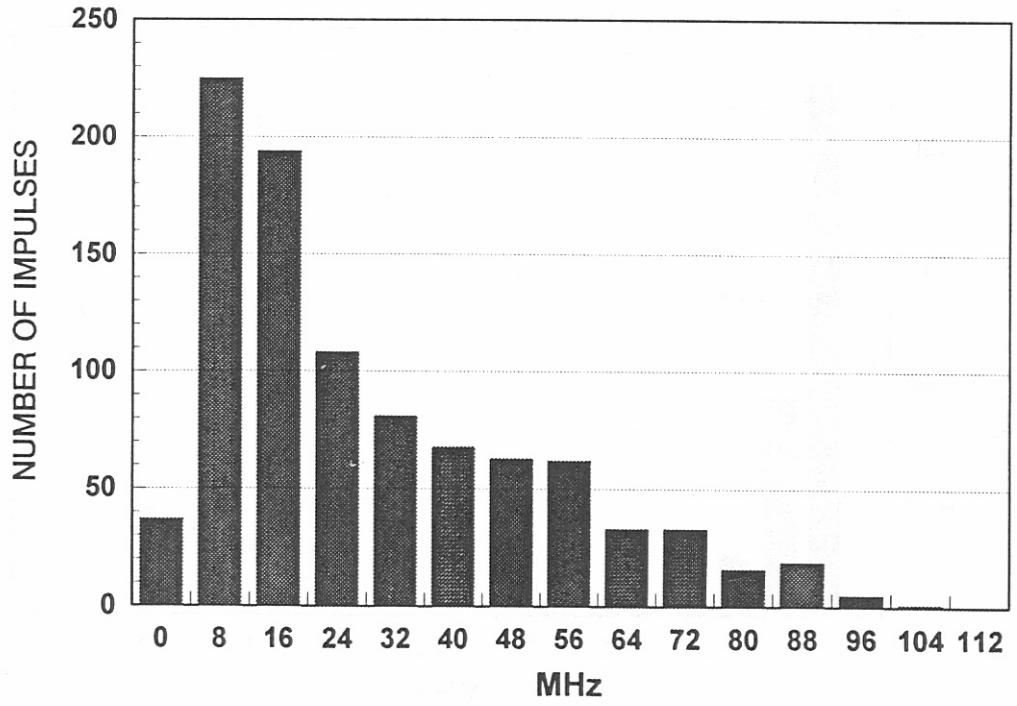

Figure 20a. Histogram of correlation BW, US WEST, LOS profiles 1 and 6.

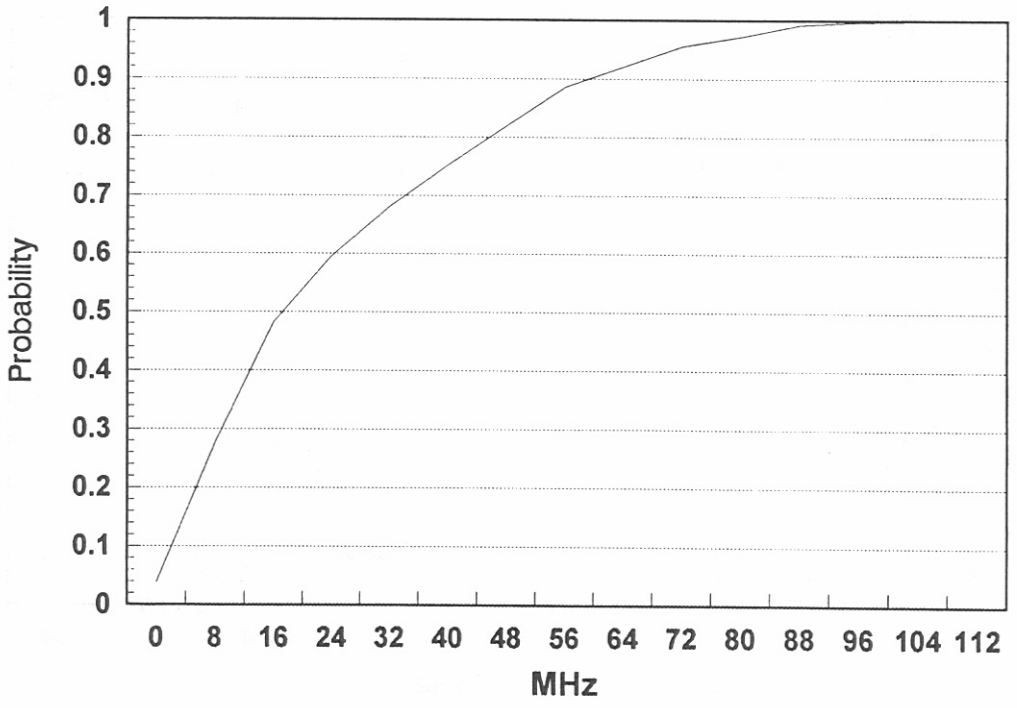

Figure 20b. CDF of correlation BW, US WEST, LOS profiles 1 and 6.

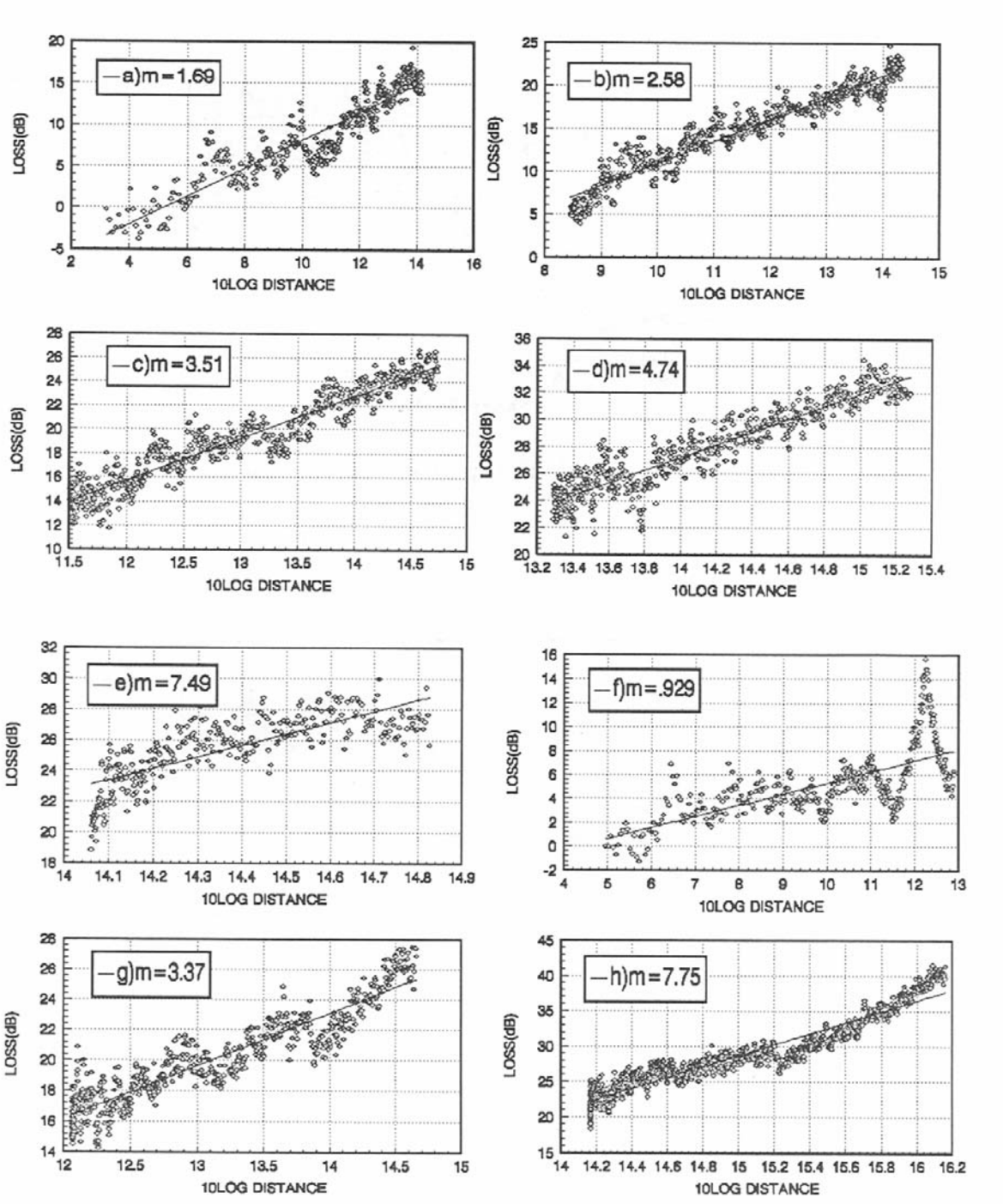

Figure 21. Attenuation scatter plots, US WEST. Profiles: (a) 1, (b) 2, (c) 3, (d) 4, (e) 5, (f) 6, (g) 7, and (h) 8.

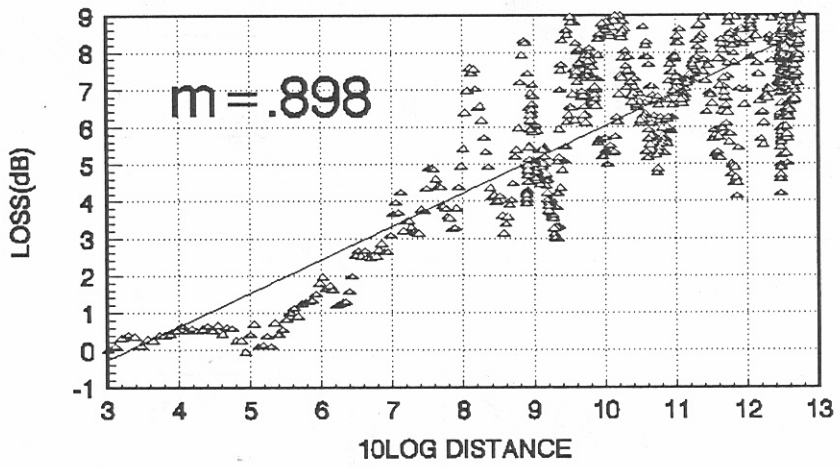

Figure 22. Attenuation scatter plot, auditorium.

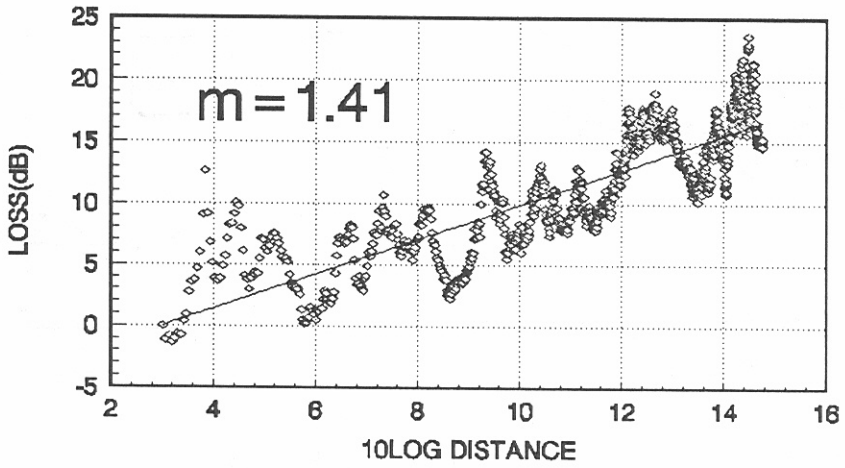

Figure 23. Attenuation scatter plot, hallway.

Table 5. Power Law Coefficients and Averages for LOS and OLOS Paths

Location	Type/#	Power Law Coefficients
DOC Hallway	LOS	1.41
DOC Auditorium	LOS	0.898
US WEST Office	LOS/1	1.69
	LOS/6	0.929
	OLSO/2	2.58
	OLSO/3	3.51
	OLSO/4	4.74
	OLSO/5	7.49
	OLOS/7	3.37
	OLOS/8	7.75
Average	LOS	1.23
	OLSO	4.91

An inspection of these coefficients shows an average below free space loss (coefficient 2) for indoor LOS paths. However, the attenuation coefficients for OLOS paths vary between 2.58 and 7.75. The larger OLOS attenuation coefficients are explained by the number of partitions blocking the line of site on each path. It can be seen from Figure 6 that path 2 has the fewest partitions separating the transmitter and receiver and the smallest attenuation coefficient for the OLOS paths. The coefficient then increases on paths 7, 3, 4, 5, and 8 as the number of partitions between transmitter and receiver increases.

6. CONCLUSIONS

The ITS wideband probe is an effective system for indoor channel measurements. In its present configuration, using a 1.5 GHz carrier and 500 Mb/s pseudo random modulation, it is well suited to study interference on proposed indoor wireless communication channels.

Standard delay spread and processing algorithms were compiled from the literature and used for data analysis. These algorithms can be used as a basis for comparison of multipath interference data with other ITS wideband measurement systems.

Data have been collected to characterize three indoor environments. At Site #1, a narrow cinderblock hallway, the median delay spread was about 7 ns and the power law loss coefficient was 1.4. At Site #2, the open auditorium, the median delay spread was 18 ns, and the power law loss coefficient was 0.9. For Site #3, the open partitioned office, the median delay spread for the OLOS data was 80 ns, and the loss coefficients ranged from 2.8 to 7.8.

This distribution of delay spreads and attenuation coefficients is consistent with the three environments. The long narrow hallway had the shortest delays due to reflections from close-in walls, the open auditorium had slightly longer delays due to reflections from distant walls, and the soft partitioned office had the longest delays due to obstructed line-of-site and highly lossy partitions.

Further study is needed to develop interpretational and modeling methods to more fully characterize indoor multipath interference effects from channel impulse response data.

7. REFERENCES

Alexander, S.E. (1982), Radio propagation within buildings at 900 MHz, *Electron. Letters, 18*, pp. 913-914.

Cox, D.C. (1972), Time and frequency domain characterizations of multipath propagation at 910 MHz in a suburban mobile-radio environment, *Radio Sci., 7*, No. 12., December, pp. 1069-1077.

Devasirvatham, D.M.J. (1987), Multipath time delay spread in the digital portable radio environment, *IEEE Comm. Magazine, 25*, June, No.6.

Proakis, J.G. (1982), *Digital Communications* (McGraw-Hill), pp. 458-500.

Violette, E.J., R.H. Espeland, and K.C. Allen (1983), A diagnostic probe to investigate propagation at millimeter wave lengths, NTIA Report 83-128, August (NTIS Order No. PB 84-104223).

Violette, E.J., R.H. Espeland, and G.R. Hand (1985), Millimeter-wave urban and suburban propagation measurements using narrow and wide bandwidth channel probes, NTIA Report 85-184 (NTIS Order No. PB 86-147741).

Violette, E.J., Felix Schwering, et al. (1988), Millimeter-wave propagation at street level in an urban environment, *IEEE Trans. Geoscience and Remote Sensing, 26*, No.3, May, pp. 355-367.

*U.S. GOVERNMENT PRINTING OFFICE: 1993-774-025/69044

FORM **NTIA-29**
(4-80)

U.S. DEPARTMENT OF COMMERCE
NAT'L. TELECOMMUNICATIONS AND INFORMATION ADMINISTRATION

BIBLIOGRAPHIC DATA SHEET

	1. PUBLICATION NO.	2. Gov't Accession No.	3. Recipient's Accession No.
	93-292		

4. TITLE AND SUBTITLE

Wideband Propagation Measurements for Wireless Indoor Communication

5. Publication Date: Jan 93

6. Performing Organization Code: *NTIA/ITS.S3*

7. AUTHOR(S) *Peter B Papazian, Yeh Lo, Elizabeth E Pol, Michael G Roadifer, Thomas G Hoople, Robert J Achatz*

8. PERFORMING ORGANIZATION NAME AND ADDRESS

U.S. Department of Commerce
NTIA/ITS.S3
325 Broadway
Boulder, CO 80303-3328

9. Project/Task/Work Unit No.: *9103108*

10. Contract/Grant No.

11. Sponsoring Organization Name and Address

U.S. Department of Commerce
NTIA
14th & Constitution AVE, NW
Washington, DC 20230

12. Type of Report and Period Covered

13.

14. SUPPLEMENTARY NOTES

15. ABSTRACT *(A 200-word or less factual summary of most significant information. If document includes a significant bibliography or literature survey, mention it here.)*

Wideband impulse response measurements were made to characterize proposed radio data channels in three indoor environments. The measurement system employed a 1.5 GHz carrier which was biphase shift key (BPSK) modulated using a 100 Mb/s pseudo-random code. By using a correlation receiver, the channel cophase and quadphase responses were measured and stored for later processing. Data processing included calculation of delay spread, correlation bandwidth (BW), and signal attenuation. The raw data are stored in binary form on tape and disk for further indoor propagation channel studies.

16. Key Words *(Alphabetical order, separated by semicolons)*

attenuation; BPSK; channel response; correlation bandwidth; delay spread; impulse response; indoor; propagation; radio; wideband

17. AVAILABILITY STATEMENT	18. Security Class. *(This report)*	20. Number of pages
☒ UNLIMITED.	*UNCLASSIFIED*	*34*
☐ FOR OFFICIAL DISTRIBUTION.	19. Security Class. *(This page)*	21. Price:
	UNCLASSIFIED	